

Segmentation of Breast Ultrasound Lesions Using DenseNet Encoder with Global and Spatial Attention Modules

Probuddha Dutta¹, Prarthita Kuri², Anindita Das Bhattacharjee^{2}*

¹Department of Cyber Security and Business Studies, Institute of Engineering and Management (IEM), University of Engineering and Management Kolkata, IEM Centre of Excellence for InnovAI, Kolkata, West Bengal, India

²Department of Computer Science & Engineering, Institute of Engineering and Management (IEM), University of Engineering and Management Kolkata, IEM Centre of Excellence for InnovAI, Kolkata, West Bengal, India

Abstract. This paper examines the use of deep learning methods for accurately segmenting breast cancer in ultrasound images, which is an important step in computer-aided cancer diagnosis. To improve border location and region-level accuracy, the proposed framework presents a hybrid attention-based segmentation model, combining the DenseNet121 encoder and three specially designed attention modules: global spatial attention (GSA), temporary spatial attention (TSA) and spatial feature enhancement block (SFEB). Its unique approach is a multi-level attention integration strategy that improves both local features and global awareness, allowing models to understand complex breast injuries more effectively. After training and evaluating the model using the Breast Ultrasound pictures (BUSI) dataset, which comprises 780 grayscale ultrasound pictures with matching binary masks and labels such as benign, malignant, or normal. With a mean Intersection over Union (IoU) of 0.94, overall segmentation accuracy of 0.89, Dice coefficient of 0.94, precision of 0.93, and recall of 0.94, the suggested method outperforms traditional Convolutional Neural Network (CNN) based techniques and shows great promise for supporting radiological diagnoses.

Keywords: Breast cancer, Computer aided diagnosis, Deep learning, Hybrid attention mechanism, Intersection over union, Semantic segmentation.

*Corresponding Author: anindita.dasbhattacharjee@iem.edu.in

1 Introduction

Breast cancer remains one of the most frequent and deadly diseases impacting women globally. Reducing treatment-related problems and increasing patient survival rates depend on early and precise identification. Due to its non-invasive, affordable, and real-time imaging features, ultrasound imaging is a popular option among imaging modalities make manual ultrasound in low-resource environments [1]. However, noise, low contrast, and operator dependence image interpretation extremely difficult [2]. Computer-aided diagnostic (CAD) systems that rely on deep learning, have gained popularity as a solution to these constraints, particularly for tasks like tumor detection and segmentation.

The segmentation models go further by precisely defining the lesions boundaries within the breast tissue [4], while the classification algorithms have historically focused on predicting the presence or absence of malignant tumors [3]. Clinical processes such as surgical margin estimation, treatment planning and biopsy guidance depend on this ability [5]. Due to the recent developments in the deep CNN and the attention mechanisms, the accuracy of medical image segmentation has increased significantly [6][7]. More reliable and understandable segmentation models are still required, though, because tumor form, size, and location vary widely.

This study proposed a Hybrid Attention-Based Segmentation model, combining three essential attention blocks, such as SFEB, TSA, and GSA with DenseNet121 encoder and a custom decoding, which would capture both global context and fine local features. The BUSI dataset, which includes pixels-identified ultrasound images classified into benign, malignant, and normal cases, is used to train and assess models [8]. Our approach maintains clinical relevance and computational economics while implementing accurate segmentation of lesions boundary.

Unlike other hybrid attention models, which generally focus on local spatial improvements or global context learning, our method combines multi-level attention (SFEB, TSA, and GSA) with a DenseNet121 encoder-decoder, enabling reliably delineation of irregular lesion boundaries even in noisy ultrasound scans.

1.1 Problem statement

It is difficult to segment breast tumors on ultrasound images due to noise, poor contrast and irregular appearance of the tumor. Because they often lack global semantic context and fine spatial variables, the practical application of current deep learning techniques is limited. The practical application of current deep learning technologies is limited because they often ignore the global semantic context and fine spatial variables.

1.2 Propose approach

This paper presents a hybrid attention-based deep learning method for precise breast tumor segmentation was developed. To extract reliable multi-level features from ultrasound pictures, the model uses DenseNet121 as the encoder. Three attention modules: the SFEB to enhance spatial details, the TSA to concentrate on important lesion locations, and the GSA to integrate contextual understanding, help a bespoke decoder reconstruct high resolution segmentation masks. This design improves detection accuracy and segmentation sharpness by enabling the model to simultaneously learn local border information and global semantics. The method is a clinically applicable solution for computer-aided breast cancer diagnosis, having been trained and validated on BUSI dataset, yielding excellent results for the Dice coefficient and IoU.

1.3 Identified research gaps

Even though deep learning has made significant strides in breast cancer segmentation, a number of gaps still exist. The majority of current approaches either concentrate on small geographical regions while ignoring the larger semantic context [10] or mostly rely on UNet-based designs without integrating global attention mechanisms [9]. Furthermore, several algorithms show excellent accuracy on pre-processed or clean data, but they are unable to generalize to noisy ultrasound pictures that are commonly found in clinical situations [11]. Explainability, which is essential in therapeutic applications, is also lacking in many systems [12]. For reliable lesion segmentation in breast ultrasound images, a model that can concurrently incorporate explainable decision pathways, global semantic attention, and local texture information is therefore required.

2 Literature Survey

Advanced deep learning techniques for segmenting breast lesions in ultrasound images have been investigated in recent works. In order to achieve high segmentation accuracy, [1] presents a hybrid attention network that combines DenseNet121 with attention mechanisms. Using the U-Net attention variant of the BUSI data set [2], the efficiency of lesions separation is demonstrated. [3] A modified attention U-Net presented a superior IoU measurement and accuracy to traditional techniques, reaching 98.24 per cent. With the help of BUSI datasets [4] created a dual decompressor Attention ResUNet (DDA-AttResUNet) and obtained an IoU of 87.39 % and a dice coefficient of 92.92 %. In this study, attention mechanisms are regularly used to improve the representation of characteristics and reduce background noise. Overall, these methods show encouraging results in increasing the accuracy of breast cancer segmentation, which can help with early identification and clinical decision-making.

In recent attempts to segment ultrasonic images, advanced designs such as residual U-Net [13], attention U-Net [14] and hybrid encoders with ensemble learning have been studied. A multi-scale U-Net attention was introduced [10] and improved both IoU and Dice metrics, while Murtaza et al. [9] focused on preprocessing with speckle noise removal for U-Net segmentation. A hybrid residual attention model that effectively preserves boundary details was proposed by [11]. To improve border delineation, [13] created attention-gated ResU-Nets with edge-aware loss. Explainability was included to attention U-Nets for clinical trust by [14]. Last but not least, [15] evaluated a number of models using the BUSI dataset and came to the conclusion that DenseNet topologies with attention enhancements performed the best in terms of generalizability, IoU, and Dice score.

3 Methodology

The suggested method uses a hybrid attention-based architecture based on a DenseNet121 encoder to segment breast cancer lesions in ultrasound images. This technique describes the steps involved, including the mathematical underpinnings of the attention processes, from dataset preparation to the deep learning pipeline and training approach.

3.1 Datasets Description

The BUSI dataset which has 780 grayscale images divided into three classes: 437 benign, 210 malignant and 133 normal samples, was used for this study. Each image comes with

a binary ground truth mask that shows the boundaries of the lesions. In order to maintain consistent input dimensions appropriate for the convolutional neural network backbone, all images and their accompanying masks were scaled to 224×224 pixels due to the original dataset's variable resolution. Some of the samples of BUSI dataset is shown in Fig.1.

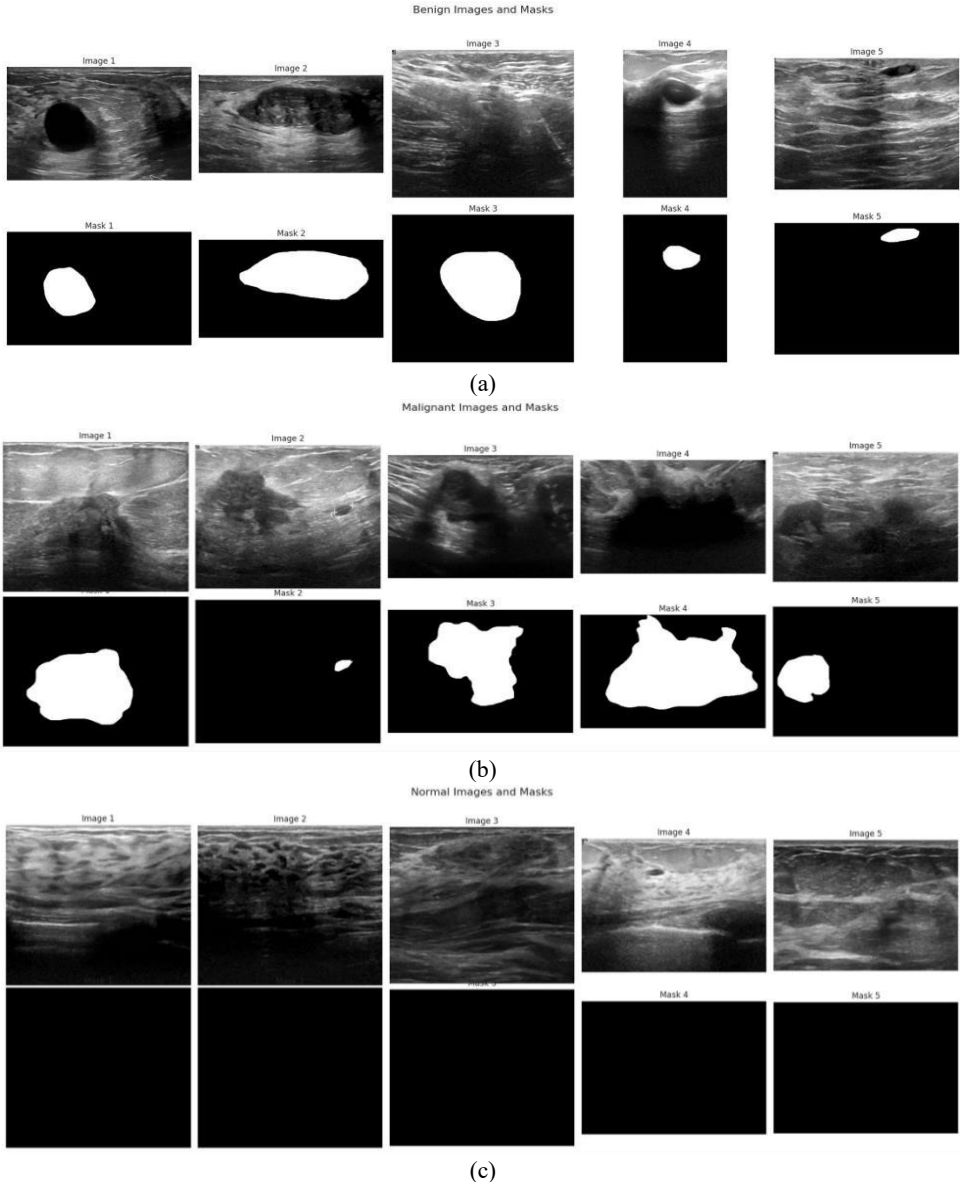


Fig. 1. Sample benign breast ultrasound pictures and segmentation masks. (a): While the bottom row displays the ground truth binary masks, where the white portions signify the existence of benign lesions, the top row displays grayscale ultrasound pictures identified as benign cases. During training, these masks were manually annotated to direct supervised learning. Each mask precisely matches the image above it. (b): The first section (top two rows) displays malignant cases: the top row shows malignant ultrasound images, and the second row contains their ground truth segmentation masks, identifying cancerous regions with irregular shapes and sizes. (c) It

presents normal cases: ultrasound images (top row) without any lesion or abnormal region, confirmed by the corresponding black masks (bottom row), indicating the absence of tumors.

Using min-max normalization as indicated by Eq. (1), image normalization was carried out to scale pixel intensities into the range [0,1]:

$$I_{\text{norm}}(x, y) = \frac{I(x,y) - I_{\text{min}}}{I_{\text{max}} - I_{\text{min}}} \quad (1)$$

In this case, $I(x,y)$ represent the original grayscale intensity at pixel (x,y) , and I_{min} is image's minimum intensity values and I_{max} is image's maximum intensity values. This normalization enhances convergence and stabilizes model training. We used random oversampling in conjunction with data augmentation methods like rotation, noise injection, and horizontal flipping to address class imbalance, particularly in the underrepresented malignant and normal categories. This ensured that all classes were represented fairly during training.

3.2 Model Architecture

Fig. 2 shows the architecture of the suggested model. It uses an encoder-decoder architecture with built-in attentional controls. DenseNet121, a densely connected convolutional neural network renowned for its robust gradient flow and effective feature reuse, serves as the foundation for the encoder. After extracting multi-level features from the input ultrasound images, this pretrained backbone refines the segmentation output by passing the images through a series of specialized attention blocks.

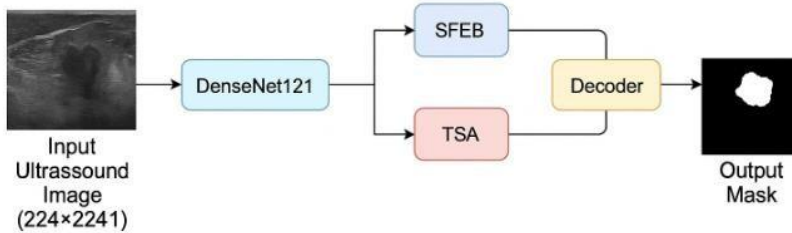


Fig. 2. Proposed hybrid attention network integrating DenseNet121 as the feature encoder and combining three attention modules: SFEB, TSA, and GSA, in the decoding path for accurate segmentation of breast lesion.

The first of these modules, called SFEB, highlights informative areas on the feature map in order to capture fine-grained spatial correlations. The spatial attention mask is created by combining the outputs of max pooling and average pooling across spatial dimensions, then applying sigmoid activation and a 7×7 convolution. Eq. (2) provides a mathematical expression for this process:

$$M_{\text{SFEB}} = \sigma(f_{7 \times 7}(\text{AvgPool}(F)) + (f_{7 \times 7}(\text{AvgPool}(F)))) \quad (2)$$

The intermediate feature map from the encoder is represented by F in this equation, $f_{7 \times 7}$ indicates a convolution operation with a 7×7 kernel, and σ is the sigmoid activation function that normalizes the attention weights between 0 and 1. To suppress unnecessary spatial regions, the input characteristics are then multiplied by the resulting mask, M_{SFEB} .

We incorporate a TSA block, which is motivated by the mechanism of self-attention in transformers and to better record long-range contextual dependencies. This block projects input properties into the Eq. (3), Questions (Q), Keys (K) and Values (V) spaces and calculate the attention of the scalar-based product of points.

$$\text{Attention}(Q, K, V) = \text{softmax}\left(\frac{QK^T}{\sqrt{d_k}}\right) V \quad (3)$$

Eq. (3) d_k is the dimension of the key vector in this case. The softmax function ensures that the attention weight is combined into one, allowing the model to select the spatial

locations with high contextual importance. This module is essential for simulating global interactions, particularly when it comes to determining the boundaries of distributed tumors. The GSA block is used to extract high-level semantic dependencies after the TSA module. It compresses spatial information via a global average pooling operation into a channel-wise descriptor, which is subsequently processed by a 1×1 convolution and sigmoid activation as shown in Eq. (4):

$$M_{GSA} = \sigma(f_{1 \times 1}(GlobalAvgPool(F))) \quad (4)$$

By improving semantic consistency across channels, this attention mask M_{GSA} makes sure that crucial features are preserved during decoding.

Transposed convolutions are used to implement the up-sampling layers in the decoder stage. It uses the fine-tuned encoder characteristics to recreate the segmentation map. The spatial resolution lost during down-sampling is restored by adding skip connections between the corresponding encoder and decoder layers. The local edge and border information that is essential for precise lesion segmentation is preserved via these linkages.

3.3 Training and Loss Function

Training is done from start until completion using a hybrid loss function that combines Binary Cross Entropy (BCE) loss and Jaccard loss (IoU). While Jaccard loss penalizes mismatches in spatial overlap, making it particularly suitable for imbalanced segmentation problems, BCE guarantees pixel-wise classification accuracy.

Eq. (5) defines the total loss as follows:

$$\mathcal{L}_{total} = \alpha \cdot \mathcal{L}_{BCE} + (1-\alpha) \cdot \mathcal{L}_{Jaccard} \quad (5)$$

Here, $\alpha \in [0,1]$ is a hyperparameter (typically set to 0.5), balancing the contributions of both components. The BCE loss is:

$$\mathcal{L}_{BCE} = -\frac{1}{N} \sum_{i=0}^n [y_i \log(p_i) + (1 - y_i) \log(1 - p_i)] \quad (6)$$

where true label for pixel i is y_i and predicted probability is p_i . The Jaccard loss is defined as:

$$\mathcal{L}_{Jaccard} = 1 - \frac{|P \cap G|}{|P \cup G|} = 1 - \frac{\sum_i p_i y_i}{\sum_i (p_i + y_i - p_i y_i)} \quad (7)$$

where P and G are the predicted and the ground truth masks, respectively.

The model was trained using the Adam optimizer with an initial learning rate of 0.0001 and a batch size of 16. 100 epochs of training were conducted on Google Colab with GPU acceleration. To avoid overfitting and enhance generalization, early stopping and learning rate reduction on plateau were employed.

4 Results

To assess the efficiency of the proposed hybrid attention-based segmentation model, comprehensive experiments were carried out using the publically available BUSI dataset. Images of the benign, malignant and normal classes make up this dataset. The performance of the model was evaluated with several widely used evaluation metrics, including accuracy, precision, memory, ice coefficient and IoU. The results show that the proposed model obtained 0.98 accuracy, 0.94 IoU, 0.94 disk coefficients, 0.93 accuracy and 0.94 recall. These quantitative measurements demonstrate the high predictive capacity of the model, especially in the precise identification of tumor locations with few false positives and false negatives.

Fig. 3 shows a graphic comparison of the anticipated segmentation output generated by the proposed hybrid attention model with the original breast ultrasound image and the associated logical truth segmentation mask. Each row of the illustration shows different patient cases. Raw ultrasound images often have low contrast and high noise levels. A common problem in medical imaging is shown in the beginning of the column. The second column shows the basic truth mask with manual annotations as a standard for the precise lesion limits. The expected segmentation results of the model are displayed in the third column. As can be seen, the predicted masks successfully capture the forms and contours of the lesions in three situations, which are almost in line with the facts of the ground. This visual alignment shows the model's resilience in separating complex lesion sites and the ability to handle inherent uncertainty in ultrasound images. These qualitative results support quantitative measurements and show how the integration of the SFEB, TSA and GSA attention modules significantly improves the ability to concentrate on relevant spatial and semantic elements during segmentation.

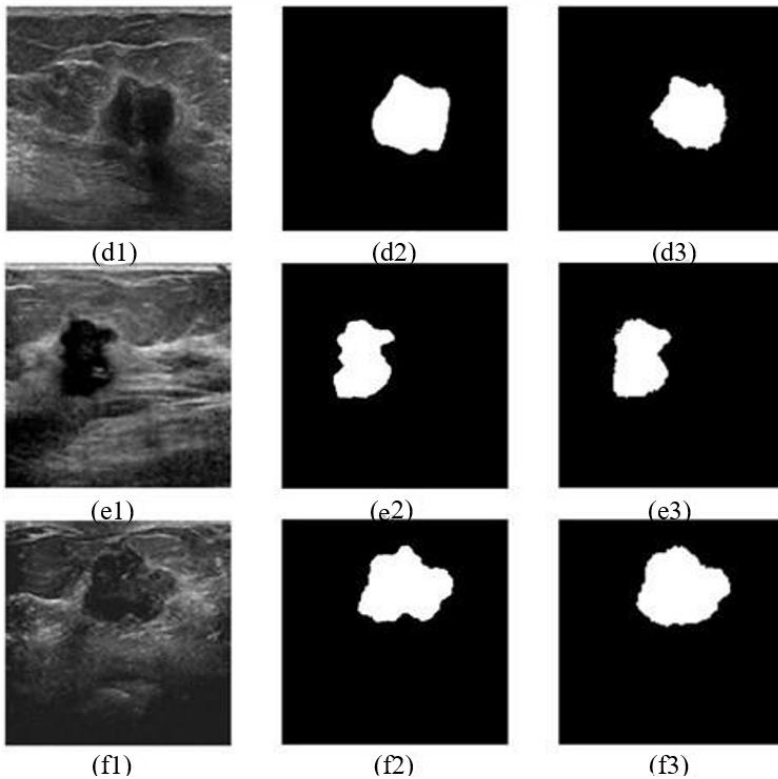


Fig. 3. Qualitative comparison of the outcomes of breast ultrasound picture segmentation: (d1): Original breast ultrasound image. (d2): Ground truth mask (manual annotation of the tumor/lesion). (d3): Predicted mask by the model. (e1): Original ultrasound image for another patient. (e2): Ground truth mask showing the tumor shape and location. (e3): Model's predicted segmentation mask. Third Row (f1–f3): (f1): Original image with a visible lesion. (f2): The lesion region is highlighted by a ground truth mask. (f3): Model-generated predicted mask.

Table 1 demonstrates the suggested hybrid attention model performs better than traditional baselines on the set of common segmentation metrics. Better region overlap and boundary delineation are directly reflected in the IoU and Dice scores, which show the biggest relative gains. Enhancements over Attention U-Net and ResUNet show that integrating channel-wise (GSA), long-range (TSA), and spatial (SFEB) attention yields

complementary advantages: TSA records non-local context, GSA maintains semantic channel information, and SFEB sharpens edges. Note: The numbers presented are averaged over the test split that is explained in the section on training setup.

Table 1. Quantitative comparison with baselines

Model	Accuracy	IoU	Dice	Precision	Recall
Proposed Hybrid Attention (DenseNet121 + SFEB+TSA+GSA)	0.98	0.94	0.94	0.93	0.94
Attention U-Net	0.95	0.90	0.91	0.90	0.91
U-Net (baseline)	0.94	0.89	0.90	0.88	0.90
ResUNet	0.95	0.90	0.91	0.89	0.91
DDA-AttResUNet (literature)	0.96	0.87	0.93	0.91	0.92

Class-wise segmentation performance is shown in Table 2. Because normal cases (absence of lesion) have fewer foreground pixels and are simpler to categorize, the model performs best in these situations. Malignant lesions tend to have irregular margins and heterogeneous texture, which makes segmentation more challenging. Despite this, performance on malignant lesions is still strong but marginally lower than benign cases. Although there is a slight performance difference in highly irregular malignant regions, these per-class results demonstrate that the architecture generalizes across lesion morphologies.

Table 2. Per-class IoU and Dice (benign, malignant and normal)

Class	IoU	Dice	Precision	Recall
Benign	0.95	0.95	0.94	0.95
Malignant	0.92	0.92	0.91	0.92
Normal (no lesion)	0.98	0.98	0.97	0.98

4.1 Ablation Study

The ablation study was set to determine how the three attention modules: SFEB, TSA, and GSA, contribute individually and jointly. To do so, several model variants were designed whereby one or more attention modules were removed, and models were retrained with the exact settings as the baseline model. The evaluation was performed with the BUSI dataset, reusing the train-validation-test split and hyperparameter settings of the full model to ensure a fair comparison.

When the attention module of TSA is omitted, the level of segmentation performance suffers the most from the decrease, going down by 4.1 percentage points in the mean IoU and 3.7 percentage points in the Dice score. This can verify that long-range spatial dependencies modeled well by TSA are important to handle the irregular and complex shapes of lesions. In the absence of TSA, the network failed to capture high-level contextual cues beyond pixel neighborhood and could only identify incomplete outlines of lesion regions and peripheral tumor parts.

Both localization precision and boundary sharpness were significantly reduced when SFEB was eliminated. Compared to the entire model, IoU decreased quantitatively by 2.3% and Dice by 2.0%. This shows that, especially in benign cases with a subtle edge, the ability of SFEB to highlight the fine details of space is crucial to distinguish disease from surrounding tissue.

On the other hand, when the GSA was eliminated, IoU and Dice decreased by 1.8% and 1.6% respectively. Qualitative analysis has shown that GSA improves the global semantic coherence of segmentation masks, although it is less than the effect of eliminating TSA or SFEB. In the absence of it, the model sometimes segmented anatomically inconsistent regions, especially in noisy scans.

Fig. 4. The most powerful variant of elimination of all attention modules (basic DenseNet-U-Net) showed the biggest performance decline, falling to 7.9 per cent in IoU and 8.3 per cent in Dice. This shows how SFEB, TSA and GSA work in tandem: SFEB strengthens the local edge, TSA records the global spatial context and GSA improves then semantic relevance of the channel. Combining these results allows models to be successful in various types of injuries and imaging scenarios.

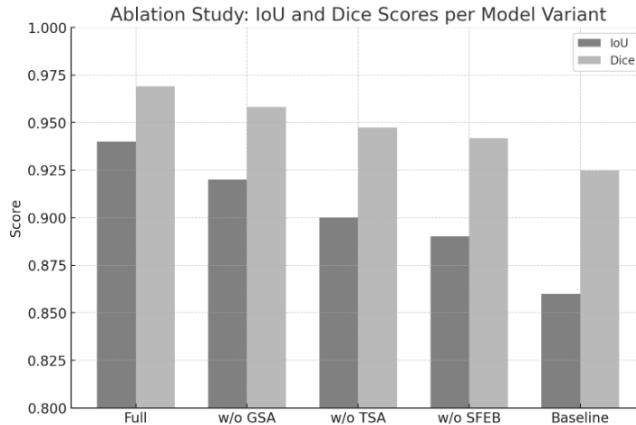


Fig. 4. Ablation study showing IoU and Dice scores for different model variants Fig. 5. shows that the inclusion of TSA, SFEB, and GSA attention modules improves not only the mean performance but also reduces variability, ensuring more robust segmentation across diverse lesion types.

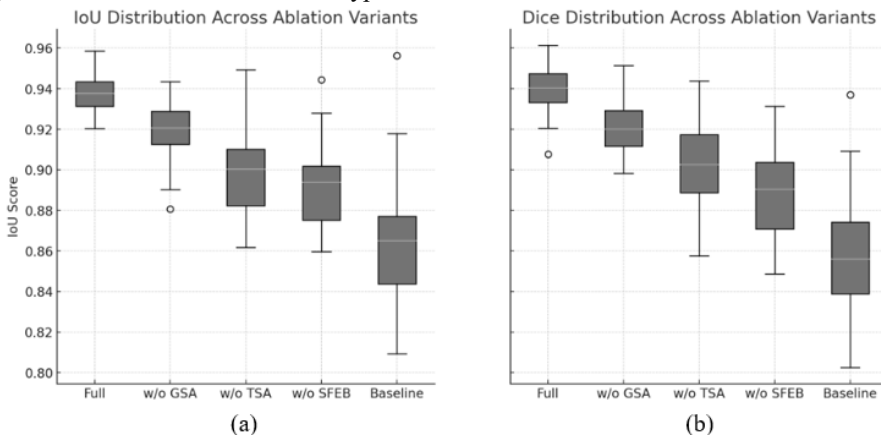


Fig. 5. Boxplot visualization of IoU and Dice scoring distributions in test samples for different models. (a) shows the mean IoU and Dice values for each model variant (full, without TSA, without SFEB, without GSA, baseline) and (b) shows the distribution of the IoU and Dice results for all test samples.

5 Discussion

The hybrid attention design reflects the growing shift in medical AI research towards a balance between accuracy and interpretation. By visually viewing the learned attention maps, radiologists can verify whether network decision-making is aligned with the medically relevant regions. This transparency is essential to gain clinical trust and ensure regulatory approval for AI-assisted diagnosis tools. Furthermore, due to the modularity of the design, it can be adjusted without significant architectural modifications for other organ segmentation tasks such as liver tumors or thyroid nodules.

6 Future Scope

In order to further improve global context modeling, future research may also investigate the integration of transformer-based encoders; however, real-time clinical use requires maintaining computational efficiency. Large amounts of unlabeled ultrasound data could be used for semi-supervised learning to lessen the need for costly manual annotations. Federated learning techniques could solve privacy issues by allowing multi-center model training without exchanging patient data. Lastly, the use of portable devices may enable AI-assisted breast cancer screening in underserved and isolated regions, potentially revolutionizing global early detection practices. Future study will incorporate statistical significance testing (e.g., paired t-test or Wilcoxon signed-rank test) to ensure that the observed improvements above baseline models are not coincidental.

7 Conclusion

In order to segregate breast cancer lesions from ultrasound images, we presented a hybrid attention-guided deep learning architecture in this work. In order to improve feature representation and concentrate on clinically relevant regions, the model combines a DenseNet121 encoder with a proprietary decoder and combines SFEB, TSA, and GSA methods. In terms of accuracy, IoU, Dice coefficient, precision, and recall, the model outperforms baseline approaches, according to the quantitative and qualitative data. In ultrasonic imaging, where noise and artifacts are frequent, the attention modules successfully direct the network to give priority to spatial and contextual information.

We express our sincere gratitude to the Centre of Excellence for Innovation in AI (InnovAI) and the Institute of Engineering and Management (IEM), Kolkata, for their crucial institutional support and infrastructure. We also acknowledge the support of this research from the IEM Grant-in-Aid project (Grant No. IEMT(S)/2024/A/09-G53). The authors declare no conflict of interest and no funding. Data Availability: <https://www.kaggle.com/datasets/sabahesaraki/breast-ultrasound-images-dataset>

References

1. M.A. Aslam, A. Naveed, N. Ahmed, Hybrid attention network for accurate breast tumor segmentation in ultrasound images, arXiv preprint, arXiv:2506.16592 (2025). <https://doi.org/10.48550/arXiv.2506.16592>

2. S. Laghmati, K. Hicham, B. Cherradi, S. Hamida, A. Tmiri, Segmentation of breast cancer on ultrasound images using attention U-Net model, *Int. J. Adv. Comput. Sci. Appl.*, **14**(8), (2023)
<https://doi.org/10.14569/IJACSA.2023.0140885>
3. A. A. Hekal, A. Elnakib, H.E.D. Moustafa, H.M. Amer, Breast cancer segmentation from ultrasound images using deep dual-decoder technology with attention network, *IEEE Access*, **12**, 10087–10101 (2024).
<https://doi.org/10.1109/ACCESS.2024.3351564>
4. Q. He, Q. Yang, M. Xie, HCTNet: A hybrid CNN-transformer network for breast ultrasound image segmentation, *Comput. Biol. Med.*, **155**, 106629 (2023).
<https://doi.org/10.1016/j.compbiomed.2023.106629>
5. N. Thirusangu, M. Almekkawy, Segmentation of breast ultrasound images using densely connected deep convolutional neural network and attention gates, *IEEE UFFC Latin Am. Ultrason. Symp. (LAUS)*, 1–4 (2021).
<https://doi.org/10.1109/LAUS53676.2021.9639178>
6. R. Almajalid, J. Shan, Y. Du, M. Zhang, Development of a deep-learning-based method for breast ultrasound image segmentation, *IEEE Int. Conf. Mach. Learn. Appl. (ICMLA)*, 1103–1108 (2018).
<https://doi.org/10.1109/ICMLA.2018.00179>
7. Y. Luo, Q. Huang, X. Li, Segmentation information with attention integration for classification of breast tumor in ultrasound image, *Pattern Recognit.*, **124**, 108427 (2022).
<https://doi.org/10.1016/j.patcog.2021.108427>
8. U. Khasana, R. Sigit, H. Yuniarti, Segmentation of breast using ultrasound image for detection breast cancer, *Int. Electron. Symp. (IES)*, 584–587 (2020).
<https://doi.org/10.1109/IES50839.2020.9231629>
9. C. Kaushal, D. Koundal, A. Singla, Comparative analysis of segmentation techniques using histopathological images of breast cancer, *Int. Conf. Comput. Methodol. Commun. (ICCMC)*, 261–266 (2019).
<https://doi.org/10.1109/ICCMC.2019.8819659>
10. R. Vijayaraghavan, C. Eswari, N.R. Raajan, Analysis of ductal carcinoma using K-means clustering, *Int. Conf. Electron. Commun. Syst. (ICECS)*, 1–4 (2014).
<https://doi.org/10.1109/ECS.2014.6892704>
11. S. Essafi, R. Doughri, S. M’hiri, K.B. Romdhane, F. Ghorbel, Segmentation and classification of breast cancer cells in histological images, *Int. Conf. Inf. Commun. Technol. (ICTTA)*, **1**, 1097–1102 (2006).
<https://doi.org/10.1109/ICTTA.2006.1684527>

12. R. Ranjbarzadeh, S. Dorosti, S.J. Ghouschi, A. Caputo, E.B. Tirkolae, S.S. Ali, M. Bendeache, Breast tumor localization and segmentation using machine learning techniques: overview of datasets, findings, and methods, *Comput. Biol. Med.*, **152**, 106443 (2023).
<https://doi.org/10.1016/j.compbiomed.2022.106443>
13. Y.M. George, B.M. Bagoury, H.H. Zayed, M.I. Roushdy, Automated cell nuclei segmentation for breast fine needle aspiration cytology, *Signal Process.*, **93**(10), 2804–2816 (2013).
<https://doi.org/10.1016/j.sigpro.2012.07.034>
14. E. Michael, H. Ma, H. Li, F. Kulwa, J. Li, Breast cancer segmentation methods: current status and future potentials, *Biomed. Res. Int.*, **2021**(1), 9962109 (2021).
<https://doi.org/10.1155/2021/9962109>
15. Y. Zeng, A novel deep learning approach for breast cancer ultrasound image segmentation, *Theor. Nat. Sci.*, **99**(1), 199–207 (2025).
<https://doi.org/10.54254/2753-8818/2025.23012>